Version 2.8.2, June 17, 2011, 3.40 pm

Evolution of the differential transverse momentum correlation function with centrality in Au+Au collisions at $\sqrt{s_{NN}} = 200$ GeV

(STAR Collaboration)

H. Agakishiev,[1] M. M. Aggarwal,[2] Z. Ahammed,[3] A. V. Alakhverdyants,[1] I. Alekseev ,[4] J. Alford,[5] B. D. Anderson,[5] C. D. Anson,[6] D. Arkhipkin,[7] G. S. Averichev,[1] J. Balewski,[8] D. R. Beavis,[7] N. K. Behera,[9] R. Bellwied,[10] M. J. Betancourt,[8] R. R. Betts,[11] A. Bhasin,[12] A. K. Bhati,[2] H. Bichsel,[13] J. Bielcik,[14] J. Bielcikova,[15] B. Biritz,[16] L. C. Bland,[7] I. G. Bordyuzhin,[4] W. Borowski,[17] J. Bouchet,[5] E. Braidot,[18] A. V. Brandin,[19] A. Bridgeman,[20] S. G. Brovko,[21] E. Bruna,[22] S. Bueltmann,[23] I. Bunzarov,[1] T. P. Burton,[7] X. Z. Cai,[24] H. Caines,[22] M. Calderón de la Barca Sánchez,[21] D. Cebra,[21] R. Cendejas,[16] M. C. Cervantes,[25] Z. Chajecki,[6] P. Chaloupka,[15] S. Chattopadhyay,[26] H. F. Chen,[27] J. H. Chen,[24] J. Y. Chen,[28] L. Chen,[28] J. Cheng,[29] M. Cherney,[30] A. Chikanian,[22] K. E. Choi,[31] W. Christie,[7] P. Chung,[15] M. J. M. Codrington,[25] R. Corliss,[8] J. G. Cramer,[13] H. J. Crawford,[32] A. Davila Leyva,[33] L. C. De Silva,[10] R. R. Debbe,[7] T. G. Dedovich,[1] A. A. Derevschikov,[34] R. Derradi de Souza,[35] L. Didenko,[7] P. Djawotho,[25] S. M. Dogra,[12] X. Dong,[3] J. L. Drachenberg,[25] J. E. Draper,[21] J. C. Dunlop,[7] L. G. Efimov,[1] M. Elnimr,[36] J. Engelage,[32] G. Eppley,[37] M. Estienne,[17] L. Eun,[38] O. Evdokimov,[11] R. Fatemi,[39] J. Fedorisin,[1] R. G. Fersch,[39] P. Filip,[1] E. Finch,[22] V. Fine,[7] Y. Fisyak,[7] C. A. Gagliardi,[25] D. R. Gangadharan,[16] F. Geurts,[37] P. Ghosh,[26] Y. N. Gorbunov,[30] A. Gordon,[7] O. G. Grebenyuk,[3] D. Grosnick,[40] S. M. Guertin,[16] A. Gupta,[12] S. Gupta,[12] W. Guryn,[7] B. Haag,[21] O. Hajkova,[14] A. Hamed,[25] L-X. Han,[24] J. W. Harris,[22] J. P. Hays-Wehle,[8] M. Heinz,[22] S. Heppelmann,[38] A. Hirsch,[41] E. Hjort,[3] G. W. Hoffmann,[33] D. J. Hofman,[11] B. Huang,[27] H. Z. Huang,[16] T. J. Humanic,[6] L. Huo,[25] G. Igo,[16] P. Jacobs,[3] W. W. Jacobs,[42] C. Jena,[43] F. Jin,[24] J. Joseph,[5] E. G. Judd,[32] S. Kabana,[17] K. Kang,[29] J. Kapitan,[15] K. Kauder,[11] H. W. Ke,[28] D. Keane,[5] A. Kechechyan,[1] D. Kettler,[13] D. P. Kikola,[41] J. Kiryluk,[3] A. Kisiel,[44] V. Kizka,[1] A. G. Knospe,[22] D. D. Koetke,[40] T. Kollegger,[45] J. Konzer,[41] I. Koralt,[23] L. Koroleva,[4] W. Korsch,[39] L. Kotchenda,[19] V. Kouchpil,[15] P. Kravtsov,[19] K. Krueger,[20] M. Krus,[14] L. Kumar,[5] P. Kurnadi,[16] M. A. C. Lamont,[7] J. M. Landgraf,[7] S. LaPointe,[36] J. Lauret,[7] A. Lebedev,[7] R. Lednicky,[1] J. H. Lee,[7] W. Leight,[8] M. J. LeVine,[7] C. Li,[27] L. Li,[33] N. Li,[28] W. Li,[24] X. Li,[41] X. Li,[46] Y. Li,[29] Z. M. Li,[28] L. M. Lima,[47] M. A. Lisa,[6] F. Liu,[28] H. Liu,[21] J. Liu,[37] T. Ljubicic,[7] W. J. Llope,[37] R. S. Longacre,[7] W. A. Love,[7] Y. Lu,[27] E. V. Lukashov,[19] X. Luo,[27] G. L. Ma,[24] Y. G. Ma,[24] D. P. Mahapatra,[43] R. Majka,[22] O. I. Mall,[21] R. Manweiler,[40] S. Margetis,[5] C. Markert,[33] H. Masui,[3] H. S. Matis,[3] Yu. A. Matulenko,[34] D. McDonald,[37] T. S. McShane,[30] A. Meschanin,[34] R. Milner,[8] N. G. Minaev,[34] S. Mioduszewski,[25] M. K. Mitrovski,[7] Y. Mohammed,[25] B. Mohanty,[26] M. M. Mondal,[26] B. Morozov,[4] D. A. Morozov,[34] M. G. Munhoz,[47] M. K. Mustafa,[41] M. Naglis,[3] B. K. Nandi,[9] T. K. Nayak,[26] P. K. Netrakanti,[41] L. V. Nogach,[34] S. B. Nurushev,[34] G. Odyniec,[3] A. Ogawa,[7] K. Oh,[31] A. Ohlson,[22] V. Okorokov,[19] E. W. Oldag,[33] R. A. N. Oliveira,[47] D. Olson,[3] M. Pachr,[14] B. S. Page,[42] S. K. Pal,[26] Y. Pandit,[5] Y. Panebratsev,[1] T. Pawlak,[44] H. Pei,[11] T. Peitzmann,[18] C. Perkins,[32] W. Peryt,[44] P. Pile,[7] M. Planinic,[48] M. A. Ploskon,[3] J. Pluta,[44] D. Plyku,[23] N. Poljak,[48] J. Porter,[3] A. M. Poskanzer,[3] B. V. K. S. Potukuchi,[12] C. B. Powell,[3] D. Prindle,[13] C. Pruneau,[36] N. K. Pruthi,[2] P. R. Pujahari,[9] J. Putschke,[22] H. Qiu,[49] R. Raniwala,[50] S. Raniwala,[50] R. L. Ray,[33] R. Redwine,[8] R. Reed,[21] H. G. Ritter,[3] J. B. Roberts,[37] O. V. Rogachevskiy,[1] J. L. Romero,[21] L. Ruan,[7] J. Rusnak,[15] N. R. Sahoo,[26] I. Sakrejda,[3] S. Salur,[21] J. Sandweiss,[22] E. Sangaline,[21] A. Sarkar,[9] J. Schambach,[33] R. P. Scharenberg,[41] A. M. Schmah,[3] N. Schmitz,[51] T. R. Schuster,[45] J. Seele,[8] J. Seger,[30] I. Selyuzhenkov,[42] P. Seyboth,[51] N. Shah,[16] E. Shahaliev,[1] M. Shao,[27] M. Sharma,[36] S. S. Shi,[28] Q. Y. Shou,[24] E. P. Sichtermann,[3] F. Simon,[51] R. N. Singaraju,[26] M. J. Skoby,[41] N. Smirnov,[22] D. Solanki,[50] P. Sorensen,[7] U. G. Souza,[47] H. M. Spinka,[20] B. Srivastava,[41] T. D. S. Stanislaus,[40] D. Staszak,[16] S. G. Steadman,[8] J. R. Stevens,[42] R. Stock,[45] M. Strikhanov,[19] B. Stringfellow,[41] A. A. P. Suaide,[47] M. C. Suarez,[11] N. L. Subba,[5] M. Sumbera,[15] X. M. Sun,[3] Y. Sun,[27] Z. Sun,[49] B. Surrow,[8] D. N. Svirida,[4] T. J. M. Symons,[3] A. Szanto de Toledo,[47] J. Takahashi,[35] A. H. Tang,[7] Z. Tang,[27] L. H. Tarini,[36] T. Tarnowsky,[52] D. Thein,[33] J. H. Thomas,[3] J. Tian,[24] A. R. Timmins,[10] D. Tlusty,[15] M. Tokarev,[1] T. A. Trainor,[13] S. Trentalange,[16] R. E. Tribble,[25] P. Tribedy,[26] O. D. Tsai,[16] T. Ullrich,[7] D. G. Underwood,[20] G. Van Buren,[7] G. van Nieuwenhuizen,[8] J. A. Vanfossen, Jr.,[5] R. Varma,[9] G. M. S. Vasconcelos,[35] A. N. Vasiliev,[34] F. Videbæk,[7] Y. P. Viyogi,[26] S. Vokal,[1] S. A. Voloshin,[36] M. Wada,[33] M. Walker,[8] F. Wang,[41] G. Wang,[16] H. Wang,[52] J. S. Wang,[49] Q. Wang,[41] X. L. Wang,[27] Y. Wang,[29] G. Webb,[39] J. C. Webb,[7] G. D. Westfall,[52] C. Whitten Jr.,[16] H. Wieman,[3] S. W. Wissink,[42] R. Witt,[53]

W. Witzke,[39] Y. F. Wu,[28] Z. Xiao,[29] W. Xie,[41] H. Xu,[49] N. Xu,[3] Q. H. Xu,[46] W. Xu,[16] Y. Xu,[27] Z. Xu,[7] L. Xue,[24] Y. Yang,[49] Y. Yang,[28] P. Yepes,[37] K. Yip,[7] I-K. Yoo,[31] M. Zawisza,[44] H. Zbroszczyk,[44] W. Zhan,[49] J. B. Zhang,[28] S. Zhang,[24] W. M. Zhang,[5] X. P. Zhang,[29] Y. Zhang,[3] Z. P. Zhang,[27] F. Zhao,[16] J. Zhao,[24] C. Zhong,[24] W. Zhou,[46] X. Zhu,[29] Y. H. Zhu,[24] R. Zoulkarneev,[1] and Y. Zoulkarneeva[1]

[1]*Joint Institute for Nuclear Research, Dubna, 141 980, Russia*
[2]*Panjab University, Chandigarh 160014, India*
[3]*Lawrence Berkeley National Laboratory, Berkeley, California 94720, USA*
[4]*Alikhanov Institute for Theoretical and Experimental Physics, Moscow, Russia*
[5]*Kent State University, Kent, Ohio 44242, USA*
[6]*Ohio State University, Columbus, Ohio 43210, USA*
[7]*Brookhaven National Laboratory, Upton, New York 11973, USA*
[8]*Massachusetts Institute of Technology, Cambridge, MA 02139-4307, USA*
[9]*Indian Institute of Technology, Mumbai, India*
[10]*University of Houston, Houston, TX, 77204, USA*
[11]*University of Illinois at Chicago, Chicago, Illinois 60607, USA*
[12]*University of Jammu, Jammu 180001, India*
[13]*University of Washington, Seattle, Washington 98195, USA*
[14]*Czech Technical University in Prague, FNSPE, Prague, 115 19, Czech Republic*
[15]*Nuclear Physics Institute AS CR, 250 68 Řež/Prague, Czech Republic*
[16]*University of California, Los Angeles, California 90095, USA*
[17]*SUBATECH, Nantes, France*
[18]*NIKHEF and Utrecht University, Amsterdam, The Netherlands*
[19]*Moscow Engineering Physics Institute, Moscow Russia*
[20]*Argonne National Laboratory, Argonne, Illinois 60439, USA*
[21]*University of California, Davis, California 95616, USA*
[22]*Yale University, New Haven, Connecticut 06520, USA*
[23]*Old Dominion University, Norfolk, VA, 23529, USA*
[24]*Shanghai Institute of Applied Physics, Shanghai 201800, China*
[25]*Texas A&M University, College Station, Texas 77843, USA*
[26]*Variable Energy Cyclotron Centre, Kolkata 700064, India*
[27]*University of Science & Technology of China, Hefei 230026, China*
[28]*Institute of Particle Physics, CCNU (HZNU), Wuhan 430079, China*
[29]*Tsinghua University, Beijing 100084, China*
[30]*Creighton University, Omaha, Nebraska 68178, USA*
[31]*Pusan National University, Pusan, Republic of Korea*
[32]*University of California, Berkeley, California 94720, USA*
[33]*University of Texas, Austin, Texas 78712, USA*
[34]*Institute of High Energy Physics, Protvino, Russia*
[35]*Universidade Estadual de Campinas, Sao Paulo, Brazil*
[36]*Wayne State University, Detroit, Michigan 48201, USA*
[37]*Rice University, Houston, Texas 77251, USA*
[38]*Pennsylvania State University, University Park, Pennsylvania 16802, USA*
[39]*University of Kentucky, Lexington, Kentucky, 40506-0055, USA*
[40]*Valparaiso University, Valparaiso, Indiana 46383, USA*
[41]*Purdue University, West Lafayette, Indiana 47907, USA*
[42]*Indiana University, Bloomington, Indiana 47408, USA*
[43]*Institute of Physics, Bhubaneswar 751005, India*
[44]*Warsaw University of Technology, Warsaw, Poland*
[45]*University of Frankfurt, Frankfurt, Germany*
[46]*Shandong University, Jinan, Shandong 250100, China*
[47]*Universidade de Sao Paulo, Sao Paulo, Brazil*
[48]*University of Zagreb, Zagreb, HR-10002, Croatia*
[49]*Institute of Modern Physics, Lanzhou, China*
[50]*University of Rajasthan, Jaipur 302004, India*
[51]*Max-Planck-Institut für Physik, Munich, Germany*
[52]*Michigan State University, East Lansing, Michigan 48824, USA*
[53]*United States Naval Academy, Annapolis, MD 21402, USA*

We present first measurements of the evolution of the differential transverse momentum correlation function, C, with collision centrality in Au+Au interactions at $\sqrt{s_{NN}} = 200$ GeV. C exhibits a strong dependence on collision centrality that is qualitatively similar to that of number correlations previously reported. We use the observed longitudinal broadening of the near-side peak of C with increasing centrality to estimate the ratio of the shear viscosity to entropy density, η/s, of the matter

formed in central Au+Au interactions. We obtain an upper limit estimate of η/s that suggests that the produced medium has a small viscosity per unit entropy.

PACS numbers: 25.75.Gz, 25.75.Ld, 24.60.Ky, 24.60.-k

Measurements carried out at the Relativistic Heavy Ion Collider (RHIC) during the last decade indicate that a strongly interacting quark gluon plasma (sQGP) is produced in heavy nuclei collisions at very high beam energies [1]. It has emerged that this matter behaves as a "nearly perfect liquid", i.e., a fluid which has a very small shear viscosity per unit of entropy [1, 2]. It is a fascinating observation that the medium produced in relativistic heavy ion collisions reaches exceedingly large temperatures, of the order of 2×10^{12} K, in stark contrast to the very low temperature, $T < 3$ K, required to achieve superfluid ^{4}He.

This conclusion is based largely on comparisons of non-dissipative hydrodynamical calculations of the time evolution of collision systems with measurements of the particle production azimuthal anisotropy characterized by the elliptic flow coefficient v_2 [2, 3] in Au+Au collisions. These calculations describe the v_2 and momentum spectra measured in Au+Au collisions at $\sqrt{s_{NN}} = 200$ GeV well at midrapidity ($|\eta| < 1.0$), low transverse momentum ($p_T < 1$ GeV/c), and for mid-central collisions (impact parameter $b \leq 5$ fm)[1, 3, 4]. A measure of fluidity is provided by the ratio of shear viscosity, η, to entropy density, s, henceforth referred to as η/s. It has been conjectured that the limit for all relativistic quantum field theories at finite temperature and zero chemical potential is close to the Kovtun-Son-Starinets (KSS) bound, $\eta/s|_{KSS} = (4\pi)^{-1} \approx 0.08$ [2, 5]. Estimates of η/s based on v_2, measured in Au+Au collisions at $\sqrt{s_{NN}} = 200$ GeV, range significantly below the viscosity per unit of entropy ratio of superfluid ^{4}He and very close to the quantum limit [2, 3, 6, 7]. Given the importance of viscosity in furthering our understanding of QCD matter, it is of interest to consider alternative measurement techniques to estimate the magnitude of η/s. Di-hadron correlation measurements in heavy ion collisions have greatly advanced the studies of hot and strongly interacting matter at RHIC [10]. Indeed, studies of correlations between low and high p_T particles have revealed the modification of away-side jets and the formation of a longitudinally elongated near-side structure, known as the ridge, in central Au+Au collisions [8]. Studies of correlations between two high-p_T particles indicate that there exist event topologies for which the away-side jet is not suppressed [11]. Meanwhile, low-p_T di-hadron correlation studies reveal rich correlation structures, particularly on the away-side [8]. However, the interpretation of these different measurements is nontrivial, and a number of competing models invoking different reaction mechanisms have been suggested to explain the data, each with relative success [9]. Thus, additional observables and measurements are required to discriminate fully among these competing models.

In this work, we present measurements of the differential extension of an integral observable C [6] in Au+Au collisions at $\sqrt{s_{NN}} = 200$ GeV. C is defined as follows:

$$C(\Delta\eta, \Delta\varphi) = \frac{\left\langle \sum_{i=1}^{n_1} \sum_{i\neq j=1}^{n_2} p_{T,i} p_{T,j} \right\rangle}{\langle n \rangle_1 \langle n \rangle_2} - \langle p_T \rangle_1 \langle p_T \rangle_2 \quad (1)$$

where $\langle p_T \rangle_k \equiv \langle \sum p_{T,i} \rangle_k / \langle n \rangle_k$ is the average momentum, the label k stands for particles from each event and the brackets represent event ensemble averages. $\langle n \rangle_k$ is the average number of particles emitted at (η_k, ϕ_k). The indices i and j span all particles in a (η_k, ϕ_k) bin. $\Delta\eta = \eta_1 - \eta_2$ and $\Delta\phi = \phi_1 - \phi_2$ are the relative pseudorapidity and azimuthal angle of measured particle pairs, respectively. C is constructed using 31 and 36 bins, respectively along the $\Delta\eta$ and $\Delta\phi$ axes. Results presented here are independent of the bin width. Similarly to correlation functions already studied at RHIC, C is sensitive to various aspects of the A+A collision dynamics. However, the explicit transverse-momentum weighting provides additional sensitivity to the collision hardness. C differs structurally and quantitatively from the observables $\langle \delta p_T \delta p_T \rangle$ [12] and $\Delta\sigma^2_{p_T}$ [13] previously reported by STAR. Differences specifically stem from the fact that C is sensitive not only to number density fluctuations, but also to p_T fluctuations, and as such reflects the magnitude of momentum current correlations [6].

This study is based on an analysis of 8×10^6 minimum bias (MB) trigger events recorded by the STAR experiment in the year 2004 (RHIC Run IV). The MB trigger was defined by requiring a coincidence signal of two zero-degree calorimeters (ZDCs) located at ± 18 m from the center of the STAR Time Projection Chamber (TPC). Collision centrality was estimated based on the uncorrected primary track multiplicity within $|\eta| < 1.0$. Nine centrality classes corresponding to 0-5% (most central), 5-10% up to 70-80% (most peripheral) of the total cross-section were used. A mean number of participants, N_{part}, is attributed to each fraction of the total cross-section using a Glauber Monte Carlo simulation [14].

The analysis is restricted to charged-particle tracks measured in the TPC with $|\eta| < 1.0$. Particles of interest for our measurement are those emerging from the bulk of the matter. Comparisons of RHIC data to hydrodynamic models show that the (near) equilibrium description only holds for particles with $p_T \leq 2$ GeV/c. For larger momenta, particle production is dominated by hard processes. Thus, we restrict this measurement to low p_T, i.e.,

with both particles in the range $0.2 < p_T < 2.0$ GeV/c. Tracks were selected on the basis of standard STAR quality cuts [15]. To minimize acceptance effects, events were analyzed provided their collision vertex lay within a distance of $|z| < 25$ cm from the center of the TPC. However, the particle acceptance exhibits a small dependence on the collision vertex position, which may introduce artificial correlations in the measurement of C. To avoid such effects, we measure C independently for forward and reverse magnetic field settings in 20 vertex-z bins of width $\Delta z = 2.5$ cm in the range $-25 < z < 25$ cm. Then we average these measurements to obtain the correlation function. Track reconstruction inefficiencies for pairs with $\Delta\eta \sim 0$, due to track crossing or merging in the TPC, are corrected for by performing a p_T and charge sign ordered analysis of these pairs. For instance, same-sign track pairs are recorded with $\Delta\phi = -|\Delta\phi|$ for $p_{T,1} > p_{T,2}$ and $\Delta\phi = +|\Delta\phi|$ otherwise. Then pair yields measured for $-1.0 < \Delta\phi < 0$, are substituted for those at $0 < \Delta\phi < 1.0$, thereby compensating for pair losses. No track-merging corrections are made for track pairs with $|\Delta\eta| < 0.032$ and $|\Delta\phi| < 0.087$ radian (bin at the origin).

Figure 1 presents the correlation function, C, for three representative collision centralities (a) 70-80%, (b) 30-40% and (c) 0-5%. Relative statistical errors range from 0.8% in peripheral collisions to 0.9% in the most central collisions at the peak of the distribution. Sources of systematic errors on the amplitude and shape of the correlation function include the collision centrality definition on the basis of primary particle multiplicity in the range $|\eta| < 1.0$, finite centrality bin width effects, loss of track reconstruction efficiency at $p_T < 0.5$ GeV/c, B-field direction, and high TPC occupancy, as well as contamination of the correlation function from weakly decaying hadrons (K^0_S, Λ), conversion electrons, and HBT correlations. A study of the effect of the centrality definition based on particle multiplicity in the range $|\eta| < 0.5$, $|\eta| < 0.75$, and $|\eta| < 1.0$ compared to that obtained with the ZDC energy reveals that the $|\eta| < 1.0$ based centrality definition least biases the shape of C at large $\Delta\eta$. Uncertainties on the correlation yield associated with centrality boundaries and bin width vary from 10% in peripheral to less than 1% in the most central collisions. Contamination from weakly decaying particles and conversion electrons is estimated to contribute less than 2% based on measured yields and known material budget of the detector. HBT effects are essentially negligible, due to the large p_T range used in the measurement.

The overall strength of C decreases monotonically from peripheral to central collisions. In 70-80% peripheral collisions, C exhibits a near-side peak centered at $\Delta\phi \sim \Delta\eta \sim 0$ and a longitudinally extended away-side structure (i.e., broad in $\Delta\eta$) at $\Delta\phi \sim \pi$. This away-side structure largely results from effects associated with momentum conservation [16]. In more central collisions, momentum conservation effects are diluted by increased particle multiplicities, and the near- and away-side observed correlation features may result from a superposition of several mechanisms possibly including resonance and cluster decays, radial flow effects, anisotropic flow effects, initial state fluctuations, and modified jet fragmentation. In mid-central collisions (30-40%), the correlation function exhibits a sizable broadening of the near-side peak and the formation of a near-side ridge-like structure, as well as a strong elliptic flow, $\cos(2\Delta\phi)$, modulation [17]. In the most central collisions (0-5%), we observe further

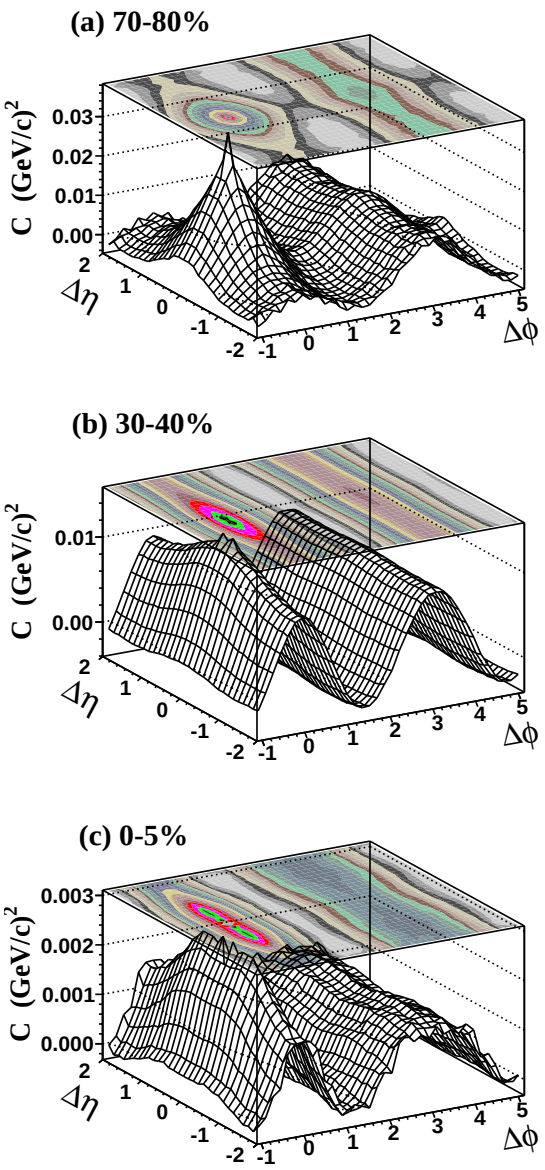

FIG. 1: (Color online) Correlation function, C, shown for (a) 70-80%, (b) 30-40%, and (c) 0-5% centrality in Au+Au collisions at $\sqrt{s_{NN}} = 200$ GeV. C is plotted in units of $(\mathrm{GeV}/c)^2$, and the relative azimuthal angle $\Delta\phi$ in radians.

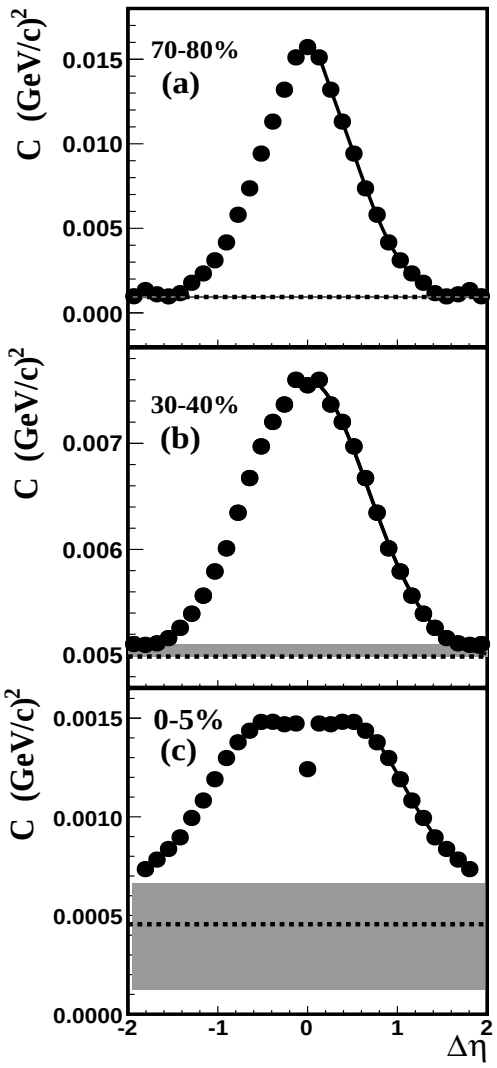

FIG. 2: (a) Projection of the correlation function C, for $|\Delta\phi| < 1.0$ radians on the $\Delta\eta$ axis for 70-80% centrality, (b) 30-40% centrality, and (c) 0-5% centrality in Au+Au collisions at $\sqrt{s_{NN}} = 200$ GeV. C is plotted in units of $(\mathrm{GeV}/c)^2$. The solid line shows the fit obtained with Eq. 2. The dotted line corresponds to the baseline, b, obtained in the fit and shaded band shows uncertainty in determining b.

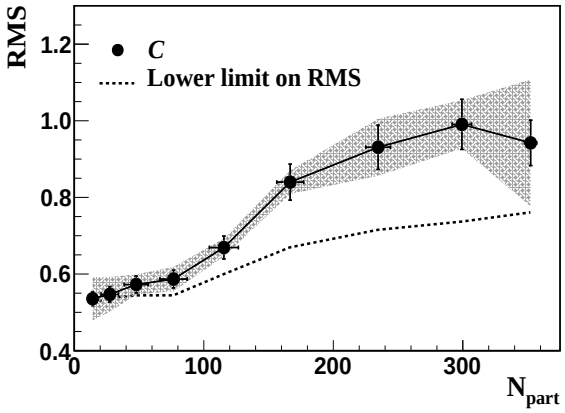

FIG. 3: RMS as function of the number of participating nucleons for the correlation function C, for nine centrality classes in Au+Au collisions at $\sqrt{s_{NN}} = 200$ GeV. The dotted line represents the absolute lower limit on RMS and shaded band represents systematic uncertainty on RMS.

longitudinal broadening of the near-side peak while the cos(2Δφ) modulation and away-side structures have a much reduced amplitude.

We next focus on the longitudinal broadening of C with increasing N_{part} based on $\Delta\eta$ projections in the range $|\Delta\phi| < 1.0$ radians. Figures 2(a-c) show the projections for 70-80%, 30-40%, and 0-5% centralities, respectively. The dip seen at $\Delta\eta \sim 0$ for 0-5% central collisions (Fig. 2(c)) is a consequence of track merging occurring at $\Delta\phi \sim \Delta\eta \sim 0$. We observe that the shape and particularly the width of the projections evolve with collision centrality. We characterize the widths of the distributions by calculating their RMS above a long range baseline, b, assumed to be constant in the acceptance of our measurement. The baseline, b, is determined using the following ansatz to fit the projections:

$$C\left(b, a_w, \sigma_w, a_n, \sigma_n\right) = b + a_w \exp\left(-\Delta\eta^2/2\sigma_w^2\right) + a_n \exp\left(-\Delta\eta^2/2\sigma_n^2\right) \quad (2)$$

where a_w and a_n stand for the amplitude of wide and narrow Gaussians with widths σ_w and σ_n, respectively.

Figure 3 shows the RMS of the correlation function as a function of N_{part}. Vertical lines reflect the statistical errors. Systematic uncertainties on the RMS are dominated by uncertainties in the baseline determination and lack of knowledge of the correlations long $\Delta\eta$ range behavior, particularly in the most central collisions. The dotted line displays the minimum RMS obtained by setting the baseline equal to the correlation yield at $\Delta\eta = \pm 2$. The gray shaded band indicates the maximum range of RMS values observed when comparing C for forward and reverse B-field, different z-bins, and various $\Delta\eta$ ranges used in the determination of the offset b. The RMS exhibits a modest increase in the range $N_{part} < 100$ which may, in part, result from long range multiplicity fluctuations and from incomplete system thermalization achieved in small collision systems. The RMS rises rapidly in the range $100 < N_{part} < 250$ after which it levels off.

According to [6], the shear viscosity should dominate the broadening of the correlation function for sufficiently large and nearly thermalized collision systems. However, jets and jet quenching could also in principle contribute to changes in the shape and broadening of the width of the correlation function with varying collision centralities. To examine this possibility, we repeated our analysis in the $0.2 < p_T < 1.0$ GeV/c and $0.2 < p_T < 20.0$ GeV/c

ranges. Our study shows that particles accepted between $0.2 < p_T < 20.0$ GeV/c produce essentially identical widths in peripheral collisions. In central collisions, RMS differs by ∼7% from the RMS widths obtained for the p_T selection $0.2 < p_T < 2.0$ GeV/c. However, lowering the upper p_T cut to 1.0 GeV/c ($0.2 < p_T < 1.0$ GeV/c) does not change the widths within statistical errors for $0.2 < p_T < 2.0$ GeV/c range for the most central collisions, and decreases the widths by ∼10% in peripheral collisions. Systematic errors are estimated based on comparisons of C obtained for different z-bins, B-field directions, and the uncertainty in determining the baseline, amounting to 10% (peripheral) to 18% (central collisions). Additionally, in a fluid, viscous effects are largest for contiguous, co-moving fluid cells. Therefore, we restricted our measurement to the particles closer in azimuth, $|\Delta\phi| < 1.0$ radians, in order to emphasize pairs of particles emerging from co-moving fluid cells. The authors of Ref. [6] argue that the longitudinal broadening of C is connected to η/s by:

$$\sigma_c^2 - \sigma_0^2 = 4\frac{\eta}{T_c s}\left(\tau_0^{-1} - \tau_{c,f}^{-1}\right) \quad (3)$$

where σ_c and σ_0 stand for the longitudinal widths of the correlation function in central collisions and at formation time, respectively. τ_0 refers to the formation time and $\tau_{c,f}$ is the kinetic freeze-out time at which particles have no further interactions [18]. T_c stands for a characteristic temperature, here taken to be the critical temperature. We proceed by assuming that viscous broadening dominates the increase in C with increasing centrality observed in this analysis and utilize Eq. 3 to estimate η/s. We estimate $\sigma_o = 0.54 \pm 0.02(stat.) \pm 0.06(sys.)$ by extrapolating the RMS width of C to $N_{part} \sim 2$. The RMS value for most central collisions is $\sigma_c = 0.94 \pm 0.06(stat.) \pm 0.17(sys.)$. Using commonly accepted estimates of 1 fm/c, 20 fm/c, and 170 MeV [19] for the formation time, central collision freeze-out, and effective temperature, we obtain a value of $\eta/s = 0.13 \pm 0.03$. Inclusion of systematic uncertainties on the widths leads to a range of $\eta/s = 0.06 - 0.21$. Figure 4 shows η/s as a function of $\tau_0^{-1} - \tau_{c,f}^{-1}$ and provides an estimate of theoretical uncertainties based on a literature survey of theoretical estimates for τ_0 and T_c. τ_0 is typically assumed to be in the range 0.6 - 1.0 fm/c (e.g., [6, 18, 20]). Here, we have assumed that the broadening of C is entirely due to viscous effects. Given that other (unknown) dynamical effects could perhaps also lead to the correlation function broadening, we conclude that our measurement provides an upper limit. Based on the systematic uncertainties of our measurement and caveats of the used theoretical model, and using the ranges $150 < T_c < 190$ MeV and $0.6 < \tau_0^{-1} - \tau_{c,f}^{-1} < 1.6$ (fm/c)$^{-1}$, we derive an upper limit of order $\eta/s \sim 0.3$.

In summary, we presented first measurements of the differential transverse momentum correlation function C from Au+Au collisions at $\sqrt{s_{NN}} = 200$ GeV. In peripheral collisions, C has a shape qualitatively similar to that observed in measurements of number density correlations, with a relatively narrow near-side peak near $\Delta\eta \approx \Delta\varphi \approx 0$ and a longitudinally broad away-side [10, 13]. We find that the near-side peak progressively broadens with increasing number of collision participants while the overall strength of the correlation function decreases monotonically. These results may be used to further constrain particle production and correlation models. We used the observed longitudinal broadening to estimate η/s of the matter formed in central Au+Au collisions. Considering systematic uncertainties in the determination of correlation widths, particularly in central collisions, and assuming somewhat conservative estimates of the temperature, formation and freeze-out times, we obtain a range of $\eta/s = 0.06$ - 0.21. This result is remarkably close to the KSS bound, $(4\pi)^{-1}$, and is consistent with results obtained from hydrodynamical model comparisons to elliptic flow data [3].

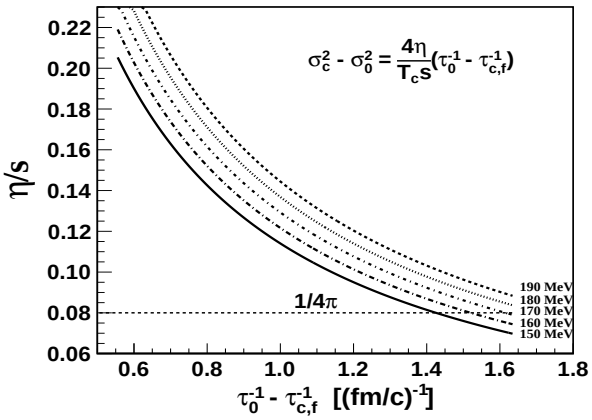

FIG. 4: η/s as a function of $\tau_0^{-1} - \tau_{c,f}^{-1}$ and T_c. τ_0 and T_c vary from $0.5 < \tau_0 < 1.5$ fm/c and $150 < T_c < 190$ MeV, respectively.

We thank the RHIC Operations Group and RCF at BNL, the NERSC Center at LBNL, and the Open Science Grid consortium for providing resources and support. This work was supported in part by the Offices of NP and HEP within the U.S. DOE Office of Science, the U.S. NSF, the Sloan Foundation, the DFG cluster of excellence 'Origin and Structure of the Universe' of Germany, CNRS/IN2P3, STFC and EPSRC of the United Kingdom, FAPESP CNPq of Brazil, Ministry of Ed. and Sci. of the Russian Federation, NNSFC, CAS, MoST, and MoE of China, GA and MSMT of the Czech Republic, FOM and NWO of the Netherlands, DAE, DST, and CSIR of India, Polish Ministry of Sci. and Higher Ed., Korea Research Foundation, Ministry of Sci., Ed. and Sports of the Rep. Of Croatia, Russian Ministry of Sci. and Tech, and RosAtom of Russia.

[1] M. Gyulassy and L. McLerran, Nucl. Phys. A **750** (2005) 30.

[2] R. A. Lacey *et al.,* Phys. Rev. Lett. **98** (2007) 092301; J. L. Nagle, I. G. Bearden and W. A, Zajc, arXiv:1102.0680 [nucl-th]; H. Song and U. W. Heinz, J. Phys. G **36**, 064033 (2009).

[3] D. Teaney, Phys. Rev. C **68** (2003) 034913; J. Phys. G **30** (2004) S1247.

[4] P. F. Kolb, P. Huovinen, U. W. Heinz and H. Heiselberg, Phys. Lett. B **500** (2001) 232; P. Huovinen *et al.,* Phys. Lett. B **503** (2001) 58; T. Hirano, Phys. Rev. C **65** (2001) 011901.

[5] G. Policastro, D. T. Son and A. O. Starinets, Phys. Rev. Lett. **87** (2001) 081601; P. K. Kovtun, D. T. Son and A. O. Starinets, Phys. Rev. Lett. **94** (2005) 111601.

[6] S. Gavin and M. Abdel-Aziz, Phys. Rev. Lett. **97** (2006) 162302.

[7] M. Issah and A. Taranenko, [PHENIX Collaboration], arXiv:nucl-ex/0604011; A. Adare *et al.,* [PHENIX Collaboration], Phys. Rev. Lett. **98** (2007) 162301.

[8] B. I. Abelev *et al.,* [STAR Collaboration], Phys. Rev. Lett. **102** (2009) 052302.

[9] N. Armesto *et al.,* Phys. Rev. Lett. **93** (2004) 242301; S. A. Voloshin, Phys. Lett. B **632** (2006) 490; M. Strickland *et al.,* Eur. Phys. J. A **29** (2006) 59; A. Majumder *et al.,* Phys. Rev. Lett. **99** (2007) 042301; E. Shuryak, Phys. Rev. C **76** (2007) 047901; A. Dumitru *et al.,* Nucl. Phys. A **810** (2008) 91; C. B. Chiu and R. C. Hwa, Phys. Rev. C **79** (2009) 034901; B. I. Abelev *et al.,* [STAR Collaboration], Phys. Rev. Lett. **103** (2009) 172301.

[10] C. Adler *et al.,* [STAR Collaboration], Phys. Rev. Lett. **90** (2003) 082302; J. Adams *et al.,* [STAR Collaboration], Phys. Rev. Lett. **95** (2005)152301; B. I. Abelev *et al.,* [STAR Collaboration], Phys. Rev. C **80** (2009) 064912; M. M. Aggarwal *et al.,* [STAR Collaboration], Phys. Rev. C **82** (2010) 024912; H. Agakishiev *et al.,* [STAR Collaboration], arXiv:1010.0690 [nucl-ex];

[11] H. Agakishiev *et al.,* [STAR Collaboration], accepted for publication in Phys. Rev C, arXiv:1102.2669v1.

[12] J. Adams *et al.,* [STAR Collaboration], Phys. Rev. C **72** (2005) 044902.

[13] J. Adams *et al.,* [STAR Collaboration], J. Phys. G**32** (2006) L37.

[14] J. Adams *et al.,* [STAR Collaboration], Phys. Rev. C **79** (2009) 034909.

[15] B. I. Abelev *et al.,* [STAR Collaboration], Phys. Rev. C **79** (2009) 024906.

[16] N. Borghini, arXiv:0707.0436.

[17] D. Teaney, Phys. Rev. C **68** (2003) 034913.

[18] J. D. Bjorken, Phys. Rev. D **27** (1983) 140; D. Teaney, Prog. Part. Nucl. Phys. **62** (2009) 451; K. Dusling *et al.,* Nucl. Phys. A **836** (2010) 159; M. Luzum and P. Romatschke, Phys. Rev. Lett. 103 (2009) 262302.

[19] T. Hirano and M. Gyulassy, Nucl. Phys. **A 769** (2006) 71.

[20] H. Song and U. Heinz, Phys. Rev. C **81** (2010) 024905.